Letter to the Editor

Adaptive optics imaging and integral field spectroscopy of APM 08279+5255: Evidence for gravitational lensing[*]

Cédric Ledoux[1], **Bertrand Théodore**[2], **Patrick Petitjean**[3,4], **Malcolm N. Bremer**[3], **Geraint F. Lewis**[5,6,**], **Rodrigo A. Ibata**[7], **Michael J. Irwin**[8], and **Edward J. Totten**[9]

[1] Observatoire Astronomique de Strasbourg, 11 Rue de l'Université, F-67000 Strasbourg, France
[2] Service d'Aéronomie du CNRS, BP 3, F-91371 Verrière le Buisson, France
[3] Institut d'Astrophysique de Paris – CNRS, 98bis Boulevard Arago, F-75014 Paris, France
[4] DAEC, Observatoire de Paris-Meudon, F-92195 Meudon Principal Cedex, France
[5] Department of Physics and Astronomy, University of Victoria, Victoria BC, Canada
[6] Astronomy Department, University of Washington, Seattle WA, USA
[7] European Southern Observatory, Karl-Schwarzschild Strasse 2, D-85748 Garching bei München, Germany
[8] Royal Greenwich Observatory, Madingley Road, Cambridge CB3 0EZ, UK
[9] Department of Physics, Keele University, Keele, Staffordshire ST5 5BG, UK

Abstract. We report observations of the $z = 3.87$ broad absorption line quasar APM 08279+5255 (Irwin et al. 1998) with the Adaptive Optics Bonnette (AOB) of the Canada-France-Hawaii Telescope. The object is found to be a double source. The separation of the two images is $0\rlap{.}''35 \pm 0\rlap{.}''02$ and the intensity ratio $I_{\mathrm{north}}/I_{\mathrm{south}} = 1.21 \pm 0.25$ in the H-band. No other image is detected down to $H(5\sigma) = 21.3$ within $10''$ from the double image. Strong support for the lensing hypothesis comes from the uniformity of the quasar spectrum as a function of spatial position in the image obtained with the integral field spectrograph OASIS at CFHT. From the 2D-spectroscopy, narrow-band images are reconstructed over the wavelength range 5600-6200 Å to search for emission-line objects in a field of $15'' \times 12''$ around the quasar. We find no such object to a limit of $6 \times 10^{-17}\,\mathrm{erg\,cm^{-2}\,s^{-1}}$. We use the images centered on the deepest absorption lines of the Lyα forest to dim the quasar and to increase the sensitivity closer to the line of sight. One of the images, centered at 5766.4 Å, exhibits a 3σ excess $1.5''$ from the quasar to the north-east.

Key words: gravitational lensing – quasars: individual: APM 08279+5255 – quasars: absorption lines

1. Introduction

Recently, Irwin et al. (1998) reported on the discovery of a highly luminous broad absorption line quasar, APM 08279+5255, at a redshift $z_{\mathrm{em}} = 3.87$, positionally coincident within one arc second with the IRAS FSC source F08279+5255. The object has an apparent R-band magnitude of 15.2 and an overall SED indicative of one of the most luminous objects of the universe, even in the probable situation that it is gravitationally lensed. Irwin et al. (1998) favored this latter explanation on the basis of a point-spread function (PSF) fitting of two discrete sources to an image of the quasar. They found a best fit with two components separated by $\sim 0\rlap{.}''4$ and an intensity ratio ~ 1.1. Several metal line systems are present in the quasar spectrum which could arise in a lensing object: a strong Mg II system at $z_{\mathrm{abs}} = 1.18$, another Mg II system at $z_{\mathrm{abs}} = 1.81$ and a damped Lyα candidate at $z_{\mathrm{abs}} = 3.07$.

Sub-mm observations with SCUBA (Lewis et al. 1998) indicate that the object contains an amount of dust comparable to that of the most luminous sub-millimeter sources at high-redshift (e.g. Downes et al. 1992; Omont et al. 1996; Petitjean 1998). This holds true even if the object is lensed. The sub-mm spectral energy distribution is consistent with emission by an optically thick black-body at a temperature of 220 K, with a minimum dust mass of 4×10^9 M$_\odot$.

In this Letter, we report adaptive optics imaging and integral field spectroscopy of the field of APM 08279+5255.

2. Observations

2.1. Adaptive optics image

We observed APM 08279+5255 using the CFHT AOB and the near-IR camera KIR on May 7, 1998 at high airmass $(sec(z) = 1.27)$. The seeing was $0\rlap{.}''8$ and the AOB correction was determined from the source itself. Four two-minutes images of the quasar were obtained in each quadrant of the detector. A background image was formed by median-averaging
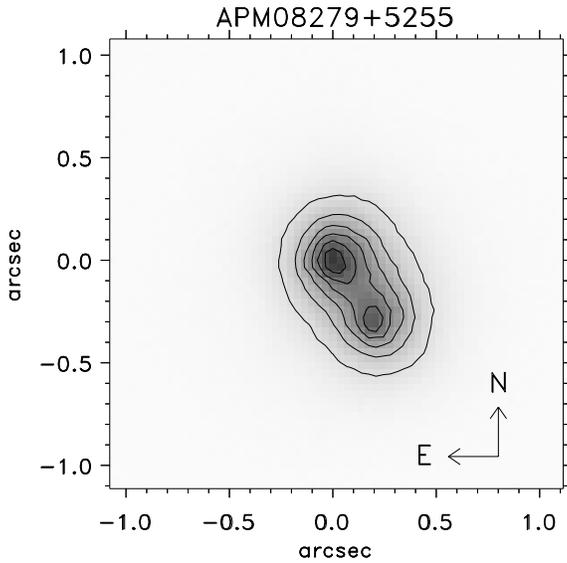
Fig. 1. PUEO-KIR H-band image of APM 08279+5255. The correction is performed on the object itself ($R = 15.2$). The total magnitude is $H = 12.6 \pm 0.1$ and the double nature of the object is apparent: the separation of the two components is $0''\!.35 \pm 0''\!.02$ and the intensity ratio $I_{\mathrm{north}}/I_{\mathrm{south}} = 1.21\pm0.25$.

these frames having excised the object from each frame. Each of the four images were flat-fielded by the normalized, dark-subtracted background frame. The images were then aligned and added together yielding the final image of resolution FWHM $\approx 0''\!.3$ shown in Fig. 1. It is apparent from this and each of the individual images that the object of total magnitude $H = 12.6 \pm 0.1$ is double. This observation strongly supports the lensing interpretation for the source put forward by Irwin et al. (1998) from deconvolution of an R-band image. More support for the lensing hypothesis comes from the uniformity of the quasar spectrum as a function of spatial position in the image obtained with the integral field spectrograph OASIS (see next Subsection).

We have used the point-spread function of a star of similar magnitude subsequently observed to subtract the two components. This procedure leaves an excess of magnitude $H > 16.5$ between the two images. The origin and reality of this excess is unclear: the stellar PSF may not be a perfect fit to the quasar PSF due to variations in weather conditions and the nearly equal flux of the two components could have led to a non-optimum AOB correction. We have therefore performed a fit to the quasar double image minimizing the chi-square between the data and a model PSF. The latter is composed of two 2D-gaussian functions assumed to reproduce the typical core plus halo structure of the PSF in the case of small Strehl ratios (see e.g. Théodore et al. 1994). The residual emission is of comparable strength to that in the stellar-PSF subtraction, but has no preferred location. Note that the residual is more than four magnitudes weaker than the quasar itself. The procedure should therefore give a reliable, although approximate, intensity ratio. From this fit, we derive that the separation between the two images is $0''\!.35 \pm 0''\!.02$ and the intensity ratio $I_{\mathrm{north}}/I_{\mathrm{south}} =$

1.21$\pm$0.25. The core and halo FWHM are $0''\!.26$ and $0''\!.64$ respectively and the intensity ratio $I_{\mathrm{core}}/I_{\mathrm{halo}} \approx 3.7$.

We have searched for additional images in a $18'' \times 18''$ field. We have detected only one non-resolved object $10''$ south-east of the lens with a 5σ magnitude of $H = 21.3$.

2.2. Integral field spectroscopy

We used the new integral field spectrograph Optically Adaptative System for Imaging Spectroscopy (OASIS) at the F/8 Cassegrain focus of the CFHT on March 29, 1998 to observe the $15'' \times 12''$ field around the quasar. The AOB correction could not be applied because of poor weather conditions; the mean seeing was $1''\!.5$ FWHM. Moreover, the sky was cloudy during the exposure making the absolute photometry uncertain. Due to the position of the object on the sky, a single 2700 s exposure was obtained. The O300 grism was used in the wavelength range 5600-6200 Å. The spectral resolution FWHM was 5.7 Å as measured on the Neon arc lines used for wavelength calibration, while the spatial scale was $0''\!.41$ per lenslet.

The data reduction was performed using the dedicated software XOasis developed by the Observatoire de Lyon (France). A set of ~ 1100 separate spectra were extracted from the CCD frame and rearranged in a 3D-datacube (α,δ,λ). During this process, an algorithm is used to compute the lens array characteristics and the distortion coefficients of the spectrograph optics. Wavelength and flat-field calibrations were consistently done with the "GUMBALL" calibration system which allows the light from the calibration source to follow the same optical path as that from the object. Cosmic ray impacts were searched for in both the spatial and spectral directions and removed.

The integrated spectrum of the quasar is shown in Fig. 2. The blue component of the Mg II absorption doublet at 6095 Å ($z_{\mathrm{abs}} = 1.1796$) is broader than its red counterpart. This is partly a consequence of blending of this line with the N V λ1242 counterpart of a N V λ1238 line seen in absorption at ≈ 6072 Å. However as the N V λ1242 line cannot be stronger than the N V λ1238 line, the Mg II doublet must be multiple to reproduce the absorption features. A fit to the doublet reveals the presence of two components separated by ~ 150 km s^{-1} and of column densities log N(Mg II) = 14.3 and 13.5 respectively. The redshift of the above N V doublet, $z_{\mathrm{abs}} = 3.9014$, indicates that part of the gas is falling towards the quasar with velocities larger than 1500 km s^{-1}.

Since the relative positions of the two images of the quasar are known from adaptive optics imaging, we have constructed two separate spectra (one for each quasar image) by selecting spectra from the lenslets that are predominantly illuminated by one of the images. The seeing during the exposure was $1''\!.5$ and the distance between the two images is only $0''\!.35$, this extraction must therefore be performed with care to lead significative results. We consider the superposition of two gaussian functions with FWHM = $1''\!.5$, intensity ratio 1.2 and separation $0''\!.35$. At a distance of $1''\!.0$ from the maximum, and in the direction joining their center, the flux of one of the components always dominates the flux of the other one by a factor larger than 2. This
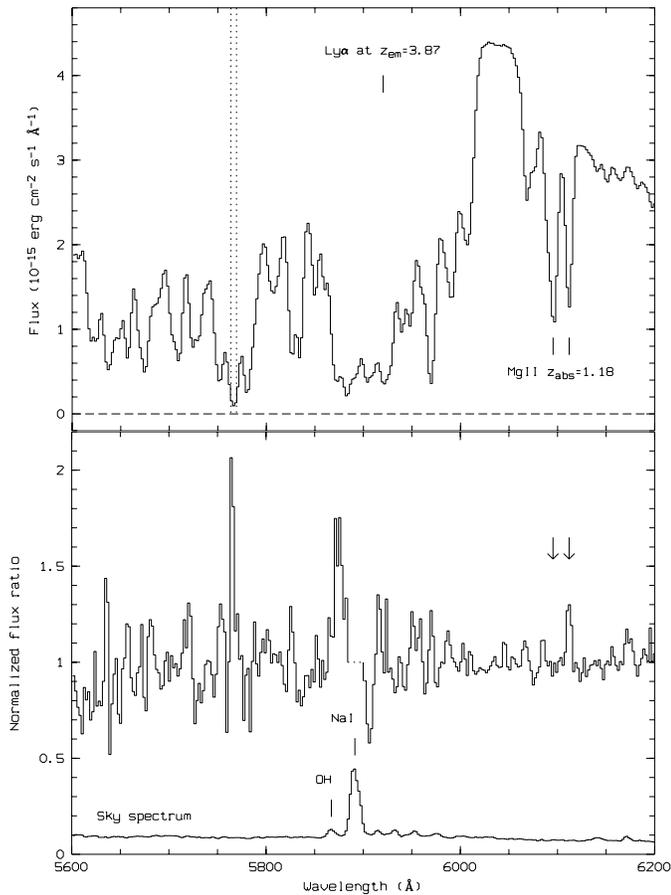
Fig. 2. Upper panel: Optical spectrum of the quasar APM 08279+5255 from integral field spectroscopy. Due to cloudy conditions, the flux calibration is uncertain by a factor 1.5. The dashed vertical lines indicate the position and width of the filter used to reconstruct the narrow-band image shown in Fig. 3. Lower panel: ratio of the north-eastern to the south-western spectra (see text for details). There is no systematic difference between the two spectra except in the Mg IIλ2803 absorption line at $z_{\rm abs} = 1.18$.

factor is even better in the north-east since the north-eastern component is stronger. We have added the spectra of 14 and 12 lenslets at a distance larger than $1\rlap{.}''2$ from the maximum (taking into account the lenslet size) and inside a radius of $0\rlap{.}''8$ in the north-east and south-west directions respectively. To avoid possible systematic errors due to the discrete 2D-spectroscopy, we have performed the same extraction on the standard star that was observed just after the science exposure. The ratio of the north-eastern to the south-western spectra corrected from the standard star is shown in Fig. 2. In the red, $\sigma = 0.1$, and it is apparent that there is no significant difference in the emission line range except at $6112\,\text{Å}$ (3σ deviation). Interesting enough, this is the wavelength of the Mg IIλ2803 absorption line at $z_{\rm abs} = 1.18$ suggesting that the doublet ratio is weaker (and so is the column density) in front of the northern image, indicative of small-scale spatial variations of the column densities in this strong system. In the Lyα forest, $\sigma = 0.25$. However, it is apparent that there is no difference in the strong broad absorptions just blueward the Lyα emission line. This altogether is a good indication that

the quasar is lensed. Indeed, if the two quasars were different, we would expect to see strong differences in the BAL as it is the case for HS 1216+5032A,B (Hagen et al. 1996). BALs are expected to arise in gas ejected by the quasar with rapid spatial variations (Monier et al. 1998). There is an apparently strong deviation at λ5885 but this is due to the presence of the very strong sky emission line. There may be a significant difference at λ5874 and λ5766 but it must be noticed that the uncertainty at these wavelengths is very large since these two wavelengths correspond to minima in the spectrum.

Using the flux-calibrated object datacube, narrow-band images of the field can be reconstructed at any wavelength within the observed range to search for line-emitting objects. Without any quasar subtraction, we find no such object to a limit of $6\times10^{-17}\,\text{erg cm}^{-2}\,\text{s}^{-1}$. The redshift range probed by our observations is 0.503-0.664 for [O II]λ3727 and 3.609-4.103 for H I Lyα. Unfortunately, the current observations do not cover the redshifts of either the candidate damped system at $z_{\rm abs} = 3.07$ (Irwin et al. 1998) or the strong Mg II system at $z_{\rm abs} = 1.18$. The quasar, although attenuated by a large factor in the Lyα forest, is still bright in most of the images however. In order to detect objects lying in projection close to the quasar, we have performed a subtraction of the residual light using the image of the quasar integrated over the whole wavelength interval and then scaled to the residual intensity in the narrow-band filter. This procedure takes into account the exact shape of the double image and, because of the scaling operation, subtracts very few of an hypothetical flat-spectrum or line-emitting object except at wavelengths where the quasar is at its maximum. This prevents however to detect sources with the same spectrum as the quasar.

No prominent line-emitting object is detected but, when performing the QSO subtraction, residual intensity is seen in a region $1\rlap{.}''5$ away from the quasar to the north-east. To check whether this residual is an artifact of the QSO subtraction or not, we can take advantage of the fact that the Lyα line at 5766.4 Å is nearly black to construct an image where the quasar is at its minimum[1]. The image in a narrow spectral band centered at 5766.4 Å and of width 5.7 Å, corresponding to the spectral resolution element (FWHM), is shown in Fig. 3 (left panel). The image obtained after subtraction of the QSO is shown in the same figure (right panel). If the excess seen $1\rlap{.}''5$ north-east of the quasar has a flat-continuum spectrum, then the R magnitude of the object is of the order of 20.6. To increase the signal-to-noise ratio in the image, we have applied the same technique for all the Lyα absorption lines. An excess is seen at the same location but with magnitude $R \sim 21$ if the spectrum is assumed to be from a flat-continuum source. Since the excess is only measured at the 3σ level and is not seen in the H-band adaptive optics image, this cannot be considered as a firm detection and additional data is needed to confirm the presence of an object.

---

[1] Note that the non-zero level in this spectral bin (see Fig. 2) is due to the low resolution of the spectrum. Profile fitting of the line shows that even for a column density as large as $\log N(\text{H I}) \sim 19.4$ and a Doppler parameter as small as $b \sim 10\,\text{km s}^{-1}$, the spectrum is not expected to go to the zero level.
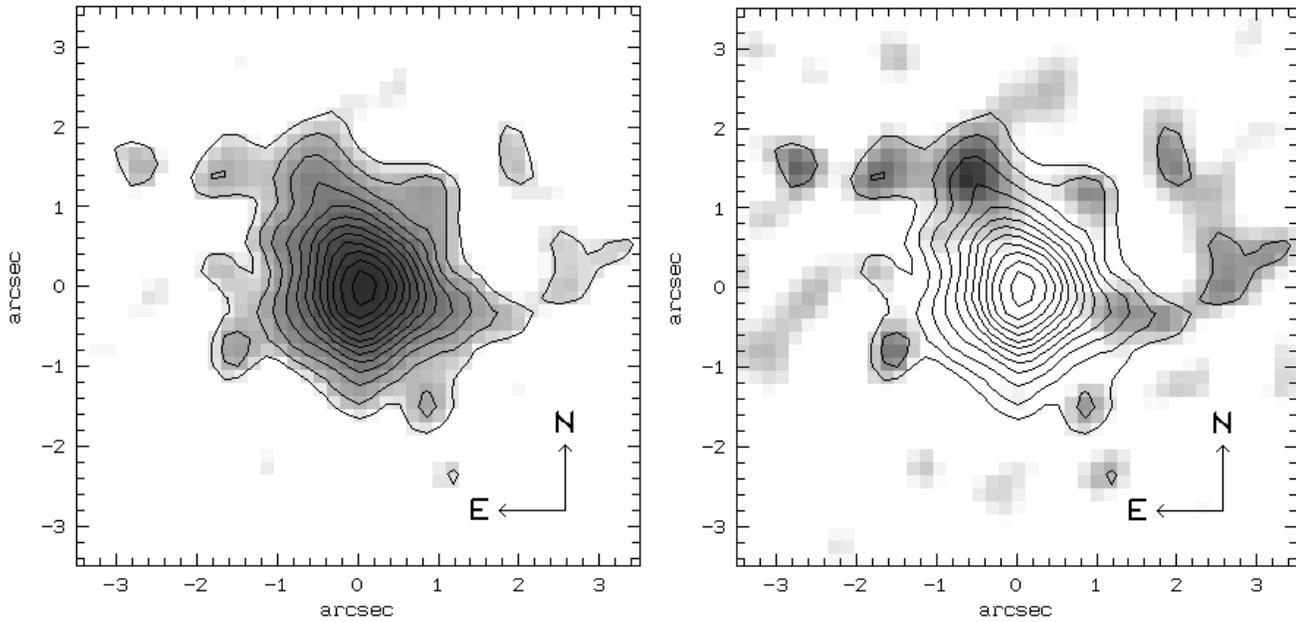
Fig. 3. Narrow-band image of the field surrounding APM 08279+5255. The central wavelength and the width of the filter are 5766.4 Å and 5.7 Å respectively, centered on the deepest Lyα absorption seen in the forest of the quasar spectrum. The left panel corresponds to the image reconstructed from integral field spectroscopy. In the right panel, the quasar image has been subtracted. The magnitude of the 3σ excess (the cut levels have been adjusted to enhance the contrast) seen $1\overset{''}{.}5$ to the north-east of the quasar is $R \sim 20.6$ if its spectrum is assumed to be flat over the R-band.

3. Conclusion

From the fit of the H-band adaptive optics image of APM 08279 +5255, we have confirmed that this quasar is double with separation between the two sources $0\overset{''}{.}35 \pm 0\overset{''}{.}02$ and an intensity ratio $I_{\mathrm{north}}/I_{\mathrm{south}} = 1.21\pm0.25$. From integral field spectroscopy, we derive that there is no systematic difference between the spectra of the north-eastern and south-western sources except possibly in the Mg IIλ2803 absorption line at $z_{\mathrm{abs}} = 1.18$. This is clear evidence that the quasar is gravitationally lensed. For the given characteristics, a simple singular isothermal sphere model implies an amplification factor of the order of 20 and a velocity dispersion of $120\,\mathrm{km\,s^{-1}}$. This amplification factor implies an intrinsic luminosity of the order of a few $10^{14}\,\mathrm{L}_{\odot}$ (see Irwin et al. 1998). The velocity dispersion is consistent with the velocity spread of an intervening Mg II absorption line system at $z_{\mathrm{abs}} = 1.18$.

An image separation of only $0\overset{''}{.}35$ implies that, either the lensing object is very compact and in between the two images, or that the source is close to a caustic of the deflection mapping. In the latter case, another faint image should be seen elsewhere in the field (see e.g. Young et al. 1980; Schneider et al. 1992). No other image is seen within $10''$ from the quasar down to $H = 21.3$. Narrow-band images centered on the strongest Lyα absorption lines in the forest and reconstructed from integral field spectroscopy show a 3σ excess of light of magnitude $R \sim 21$ (assuming a flat-continuum spectrum) at $1\overset{''}{.}5$ north-east of the quasar. However the reality of the source is not secure given the poor weather conditions during the observations.

It is intriguing that the broad absorption spread over more than 50 Å around 5900 Å does not go to the zero level. This indicates that it is not continuous and should split into numerous narrower components at high resolution. The presence of N V absorption at 6072 Å indicates the presence of associated systems with redshifts larger than the emission redshift of the quasar by at least 1500 km s^{-1}.

References

Downes D., Radford J. E., Greve A., Thum C., Solomon P. M., Wink J. E., 1992, ApJ 398, L25
Hagen H.-J., Hopp U., Engels D., Reimers D., 1996, A&A 308, L25
Irwin M. J., Ibata R. A., Lewis G. F., Totten E. J., 1998, ApJ 505, 529
Lewis G. F., Chapman S. C., Ibata R. A., Irwin M. J., Totten E. J., 1998, ApJ 505, L1
Monier E. M., Turnshek D. A., Lupie O. L., 1998, ApJ 496, 177
Omont A., Petitjean P., Guilloteau S., McMahon R. G., Solomon P. M., Pécontal E., 1996, Nat 382, 428
Petitjean P., 1998, in E. Corbelli, D. Galli, F. Palla (eds.), H$_2$ molecules in the early universe, in press, astro-ph/9804257
Schneider P., Ehlers J., Falco E. E., 1992, in Gravitational Lenses, Springer: Berlin
Théodore B., Petitjean P., Hubin N., 1994, The Messenger 77, 20
Young P., Gunn J. E., Kristian J., Oke J. B., Westphal J. A., 1980, ApJ 241, 507